

Comparative Analysis of Dual Active Bridge Isolated DC to DC Converter With Buck-boost and Flyback Converters for Bidirectional Energy Transfer

A.KUMAR

Research Scholar, Department of Electrical Engineering
National Institute of Technology, Srinagar
Jammu & Kashmir, India
kanupam310@gmail.com

A.HAMID BHAT

Associate Professor, Department of Electrical Engineering
National Institute of Technology, Srinagar
Jammu & Kashmir, India
bhatdee@nitsri.net

P.AGARWAL

Professor, Department of Electrical Engineering
Indian Institute of Technology, Roorkee
Uttarakhand, India
pramgfee@iitr.ac.in

Abstract: Bidirectional energy transfer capability is the central part of a lot of modern power conversion systems. Preferably, for reduction of size, weight and cost these systems use a single high efficiency power electronic conversion system. A dual active bridge converter having two DC-AC converters connected back to back through an AC inductor/transformer is a common topology used for obtaining high efficiency bidirectional power conversion. Some characteristic features of the Dual Active bridge (DAB) converter topology are bidirectional power flow capability, inherent soft switching, high power density, high efficiency, galvanic isolation and reduced number of passive components. In this paper, comparative study of Dual active bridge converter is done with conventional buck-boost and flyback converters. Also efficiency of these three converters are compared. Switching of devices for three converters is also shown. Flyback converter is operated in both buck as well as boost mode. DAB is simulated in SPS (Single phase shift) and EPS (Extended phase shift) mode

Keywords: Dual active bridge converter, bidirectional power flow, single phase shift, extended phase shift, closed loop control, PI controller, buck-boost converter, flyback converter.

1. Introduction

In modern times, the bidirectional energy transfer capability has become the central part of a lot of modern power conversion systems. For the purpose of increasing, decreasing or channelizing voltage and for maintaining a bidirectional power flow between a storage element and DC voltage bus, bidirectional DC-DC converter (BDCs) [1,2] have become very common at power electronics and industrial applications such as renewable energy systems, transportation vehicles industry, HVDCs [3] portable electronic equipments, microgrids [4] and many power applications [5] which require an intermediate energy storage system [6-7]. One such application is shown in Fig-1, the application of Dual active bridge converter in DC micro grid [8]. Advanced versions of DAB are also developed for meeting energy conversion purposes [9].

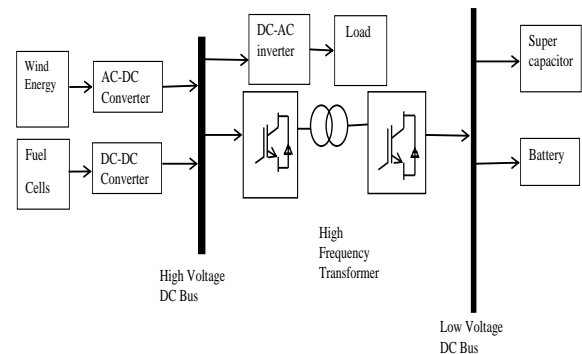


Fig.1. Dual active bridge converter in DC Micro-grid

Many researchers have worked for improving system efficiency of the BDCs and these studies are mostly related to phase shift control methods and their different variations [10]. Basically Dual active bridge (DAB) converters were first proposed in early 1990s. However the efficiency was low and due to high power losses no advancement could be made and thus the literatures related to these converters were very few. The most common method used for phase shift control is Single phase shift (SPS) control. After this for improvement of system efficiency, extension of Zero Voltage switching(ZVS) operating range [11], extended phase-shift control (EPS) [12], dual phase-shift control (DPS) [13-14] and triple phase-shift control (TPS) [15] are used and studied in detail. DAB converters have inherent soft switching capability [16] but the operating range decreases under light load conditions. However if the voltage amplitude of the two sides of the transformer do not match, then it leads to a decrement in efficiency and increment in circulating current. Dual active bridge converters can also be used in bidirectional power flow in custom power devices (UPQC etc)[17], for mitigation of power quality problems [18,19]. Also three phase topologies and multilevel topologies [20] are possible for dual active bridge converter and have been successfully implemented.

Buck and boost converters are the base of any bidirectional DC-DC Converters, the bidirectional buck-boost converters are derived from these two converters, these converters fall into the category of non-isolated bidirectional dc-dc converters. The non-isolated types include the buck-boost type, cuk type, coupled-inductor type, multi-level type, switched-capacitor type, sepic/zeta type converters. For providing large voltage gain in multilevel type converters more switches and capacitors are required. The control logic for these converters is also complicated. In case of these converters, due to connection of two power stages, the conversion efficiency is lower. The circuit structure of buck-boost converter is very simple but it is having a demerit that it does not provide wide voltage conversion range.

The flyback converter is of isolated type converter. Various other isolated converters are, forward-flyback type [21-25] and full-bridge type [26-27]. In these converters, by adjusting the turns ratio of isolation transformer, large voltage gains can be achieved. The circuit structure is quite simple and control is also easy in these converters. The drawback of these converters is that high voltage stress appears on the switches. Thus these converters are used for low power applications only.

In this paper, circuit operation, design, comparison of efficiency and closed loop operation of DAB in SPS and EPS mode is performed with flyback and bidirectional buck-boost converters. Various control strategies like single phase shift (SPS), extended phase shift (EPS) are compared and respective waveforms for DAB, flyback and buck boost converter are shown. By extensive simulation studies in MATLAB/Simulink and SimPowerSystem software, the above control strategies and converters are tested and results are obtained for a comprehensive comparative evaluation.

2. Basic operating principle of DAB, Buck-boost, Flyback Converters

Single phase dual active bridge converter is shown in Fig-2 and various switches and diodes are numbered accordingly. As shown in the figure, it consists of two back to back connected DC/AC converters connected through a high frequency transformer. The primary side leakage inductance and the secondary leakage inductor is referred to the primary side.

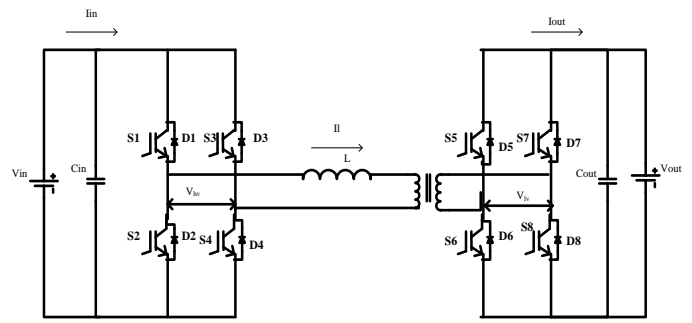
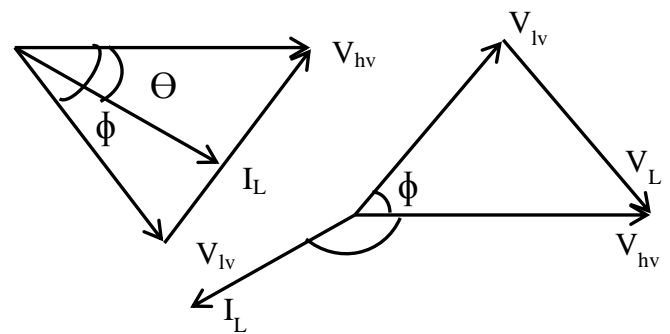


Fig.2. Power circuit diagram of single-phase dual active bridge converter

Each bridge is operated with a duty ratio of 50%. Also a high frequency square wave is generated at the transformer terminals; the two square waves can be shifted to control the direction of power flow. Phasor diagram for both the modes i.e, charging (forward power flow) as well as discharging (reverse power flow) are shown in Fig-3.

Here, V_{lv} is voltage on secondary side, V_{hv} is voltage on primary side, I_L is inductor current, Θ is phase displacement between V_{hv} and I_L , ϕ is the controlled duty ratio and is the angle or phase shift between the primary side voltage (V_{hv}) and Secondary side voltage (V_{lv}). The duty ratio(D) of dual active bridge converter is defined as $D = \Phi/\Pi$, where Φ corresponds to t_{on} and Π corresponds to half of the switching period ($T_s/2$)



(a) Forward power flow mode (b) Reverse power flow mode

Fig.3. Phasor diagram in (a) Forward power flow mode (b) Reverse power flow mode

2. (a) Single phase shift (SPS) control

The waveform for single phase shift control is shown in Fig-4:

Time interval t_0, t_1 :

Equivalent circuit is shown in Fig-5;

Governing equations are written below;

$$V_i = V_o + V_o/n \quad (1)$$

V_i =Inductor Voltage, V_i =Input voltage, V_o =output

voltage, n =transformer ratio

$$L di/dt = V_i + V_o/n \quad (2)$$

i_l =Inductor current, L = Leakage inductance of primary plus referred value of secondary leakage inductance on primary side..

$$di/dt = (V_i + V_o/n)/L \quad (3)$$

therefore di/dt is positive.

Time interval t_2, t_3 :

Equivalent circuit is shown in Fig-6;

$$V_l = V_i - V_o/n, \quad (4)$$

Governing equations are written below;

V_l =Inductor Voltage, V_i =Input voltage, V_o =output voltage, n =transformer ratio.

$$L di/dt = V_i - V_o/n; \quad (5)$$

$$di/dt = (V_i - V_o/n)/L, \quad (6)$$

Three cases arise for this time ,

Case (a) $V_i > V_o/n$ (buck mode operation)

Therefore, di/dt is positive

Case (b) $V_i = V_o/n$ leads to constant current .

Case (c) $V_i < V_o/n$ (boost mode)

Therefore di/dt is negative.

Time interval t_3-t_5 :

Equivalent circuit is shown in Fig-7;

$$V_l = -(V_i + V_o/n) \quad (7)$$

$$di/dt = -(V_i + V_o/n)/L, \quad (8)$$

Therefore di/dt is negative.

Time interval t_5-t_6 :

Equivalent circuit is shown in Fig-8.

Governing equations are written below;

$$V_l = -V_i + V_o/n; \quad (9)$$

$$L di/dt = -V_i + V_o/n; \quad (10)$$

$$di/dt = (-V_i + V_o/n)/L \quad (11)$$

Therefore di/dt is negative.

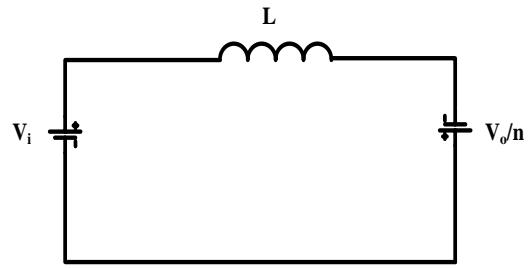


Fig.5. Equivalent circuit of DAB during time interval t_0

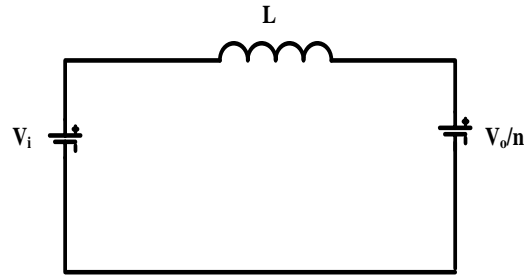


Fig.6. Equivalent circuit of DAB during time interval t_2, t_3

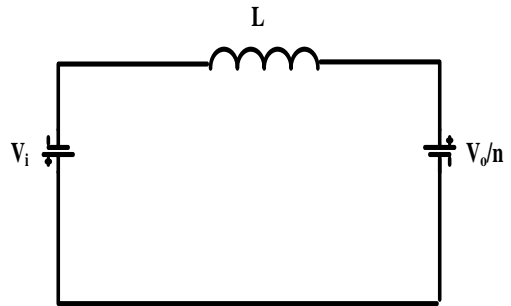


Fig.7. Equivalent circuit of DAB during time interval t_3, t_4

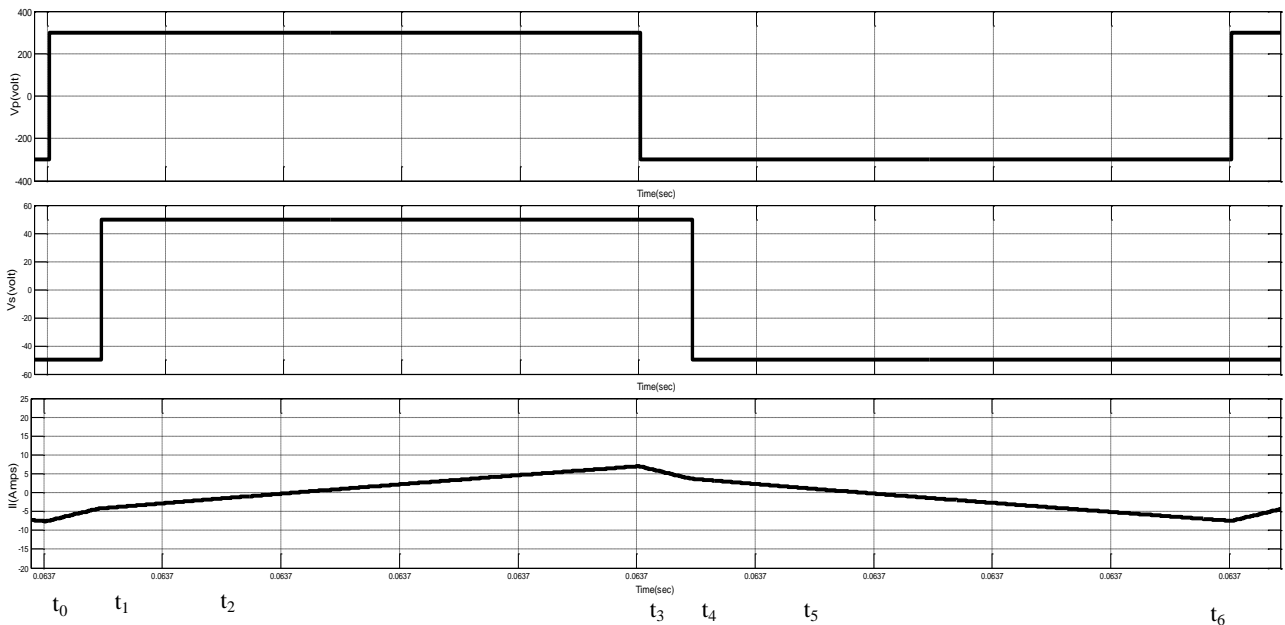


Fig 4.(a) Primary voltage(b)Secondary voltage (c) Inductor current for forward power flow.

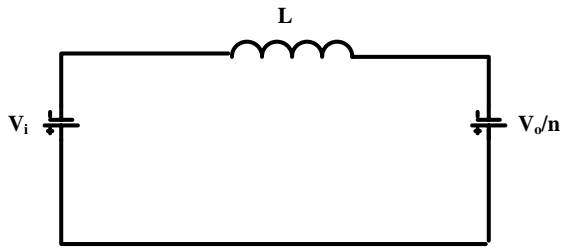


Fig.8. Equivalent circuit of DAB during time interval t_5-t_6

Similarly the waveforms can be seen in Fig-9 for reverse power flow mode. The conduction of various devices in charging as well as discharging mode is shown in table I(a) and table I (b).

Also the primary voltage, secondary voltage, inductor voltage and inductor current are shown in Fig-10 and Fig-11 for forward as well as reverse mode respectively

Table I(a)
Conduction table for forward power flow

Time interval	Device conducting in primary bridge	Device conducting in secondary bridge
t_0-t_1	D1-D4	D5-D8
t_1-t_2	S1-S4	S5-S8
t_2-t_3	S1-S4	D6-D7
t_3-t_4	D2-D3	D6-D7
t_4-t_5	S2-S3	S7-S6
t_5-t_6	S2-S3	D5-D8

Table I(b)
Conduction table for reverse power flow

Time interval	Device conducting in primary bridge	Device conducting in secondary bridge
t_0-t_1	D2-D3	D6-D7
t_1-t_2	S2-S3	S7-S6

t_2-t_3	D1-D4	S7-S6
t_3-t_4	D1-D4	D5-D8
t_4-t_5	S1-S4	S5-S8

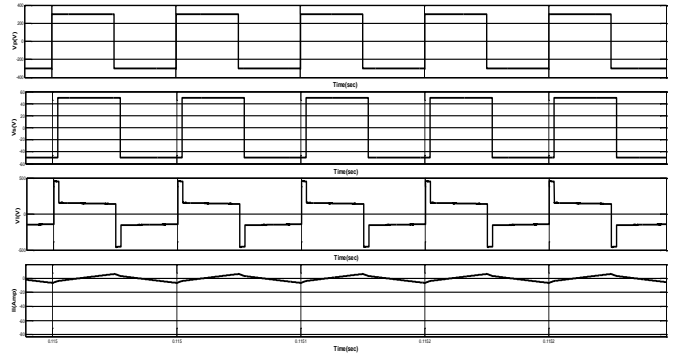


Fig.10.(a) Simulated Primary voltage, (b)Secondary voltage, (c)Inductor voltage,(d) Inductor current for forward power flow.

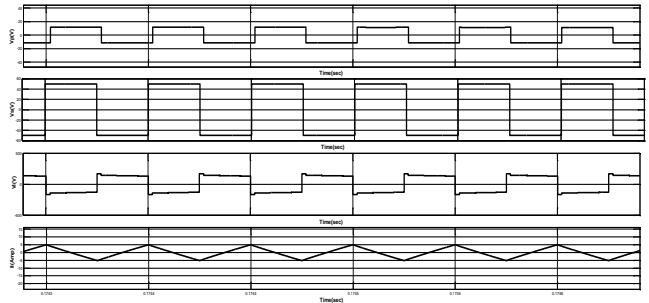


Fig.11.(a) Simulated primary voltage (b) Secondary voltage, (c) Inductor voltage, (d) Inductor current for reverse power flow

2.(b). Extended phase shift (EPS) control

For overcoming the deficiencies of SPS control strategy, EPS control is used. In EPS control the switch pairs in one bridge are provided with inner phase shift while other switch pairs are switched as before with outer phase shift only. As a result of this the primary side voltage becomes a

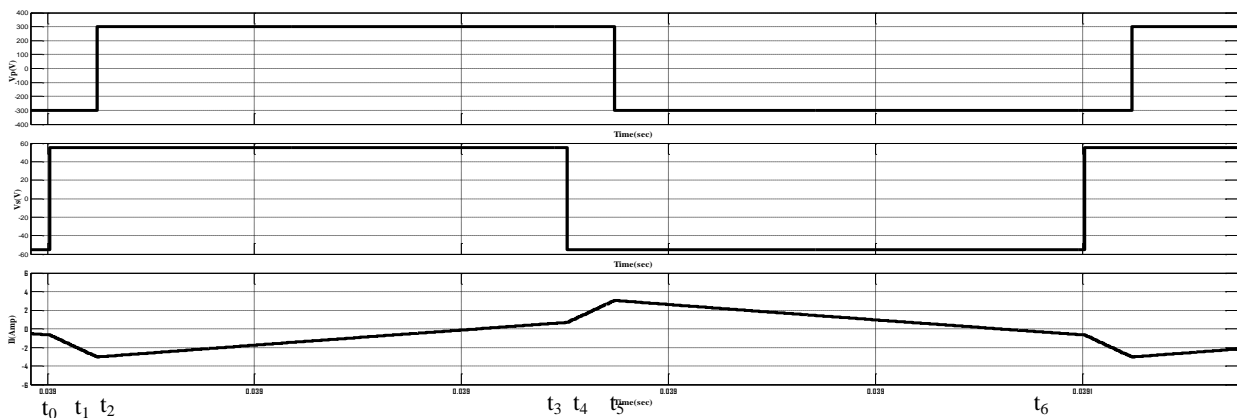


Fig.9.(a)Primary voltage (b)Secondary voltage (c)Inductor current for reverse power flow

three level wave and waveform on secondary side becomes two level wave having 50% duty ratio. In reverse conduction mode, the waveshapes of both the voltages are reversed.

The operating principle and performance of EPS has been discussed by many researchers. Analysis of EPS can be done in the same way as for SPS technique discussed above.

Also the waveforms for EPS technique in forward and reverse conduction mode are shown in Fig-12 and Fig-13.

The conduction of various devices in charging as well as discharging mode is shown in table II(a) and tableII (b).These tables are obtained from Fig-12 and Fig-13.

Table II(a)

Conduction table for forward power flow

Time interval	Device conducting in primary bridge	Device conducting in secondary bridge
t_0-t_1	D1-S3	D5-D8
t_1-t_2	S1-D4	S5-S8
t_2-t_3	S1-S4	S5-S8
t_3-t_4	S1-S4	D7-D6
t_4-t_5	D2-S4	D7-D6
t_5-t_6	S2-D4	S7-S6
t_6-t_7	S2-S3	S7-S6
t_7-t_8	S2-S3	D5-D8

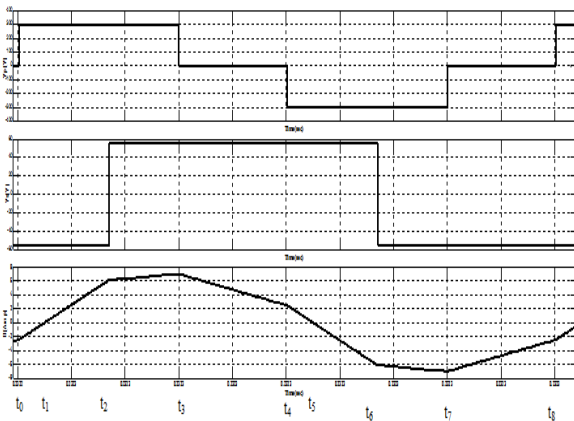


Fig.12.(a)Simulated Primary voltage (b) Secondary voltage (c)Inductor current for forward power flow

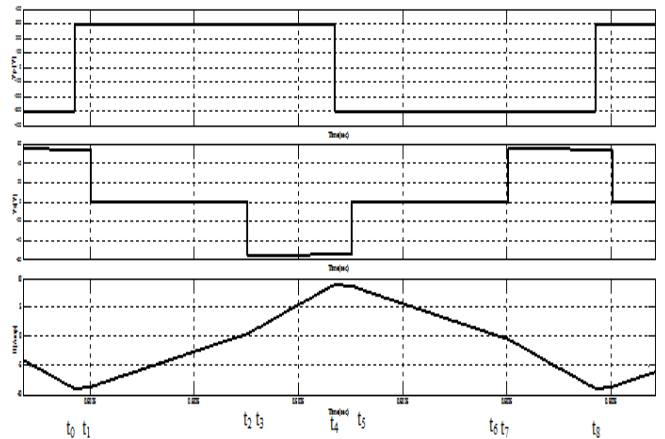


Fig.13.(a)Primary voltage (b)Secondary voltage(c)inductor current for reverse power flow

Table II(b)

Conduction table for reverse power flow

Time interval	Device conducting in primary bridge	Device conducting in secondary bridge
t_0-t_1	D1-D3	S7-S6
t_1-t_2	D1-D3	S6-D8
t_2-t_3	S1-S4	S8-D6
t_3-t_4	S1-S4	S5-S8
t_4-t_5	D2-S4	S5-S8
t_5-t_6	D2-S4	S5-D7
t_6-t_7	S2-S3	D5-S7
t_7-t_8	S2-S3	S7-S6

Also the primary voltage, secondary voltage, inductor voltage, inductor current, input current and output current are shown in Fig-14 and Fig-15 for forward as well as reverse mode respectively. The EPS as compared to SPS has better efficiency, lower switch stress and large ZVS(zero voltage switching) operating range.

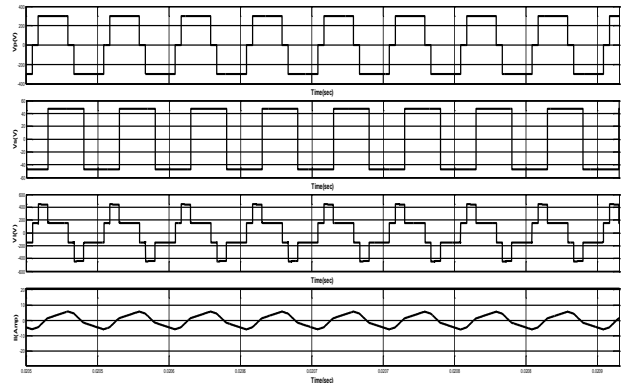


Fig.14.(a) Simulated primary voltage, (b) Secondary voltage, (c) Inductor voltage, (d) Inductor current, for forward power flow.

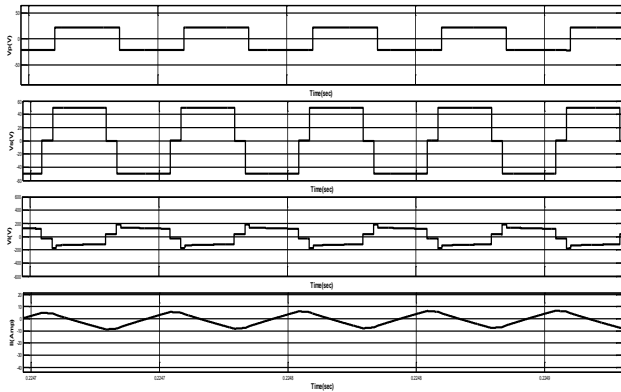


Fig.15.(a) Simulated Primary voltage, (b) Secondary voltage, (c) Inductor voltage, (d) Inductor current, for reverse power flow.

2(c). Flyback converter

A bidirectional flyback converter is shown in Fig 16. As shown in the diagram, it consists of two DC source connected with each other in opposite polarity with the help of an isolation transformer. Also the primary side current and secondary side current for boost mode is shown in fig.17. Again, the primary side current and secondary side current for buck mode is shown in fig.18.

In forward direction of power flow $V_1, S_1, D_1, Load_1, C_{f1}$ conduct and power flow is maintained in forward direction. Similarly for reverse direction $V_2, S_2, D_2, Load_2, C_{f2}$ conduct and power flow is maintained in reverse direction

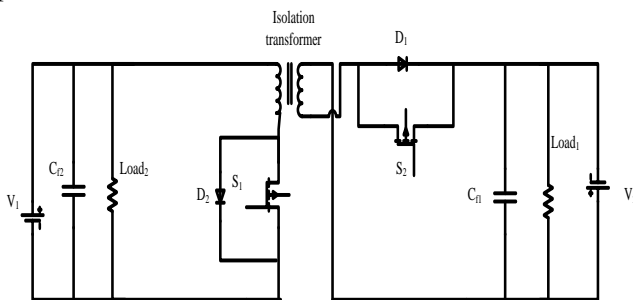


Fig.16. Power circuit diagram of a bidirectional flyback converter

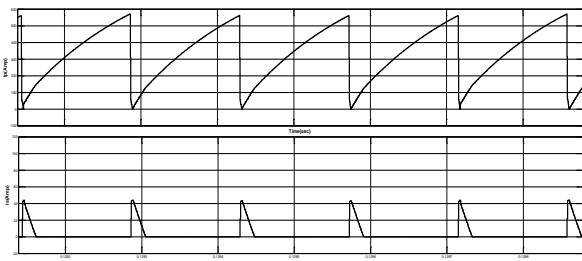


Fig.17. Simulated a) Primary current b) Secondary current in boost mode.

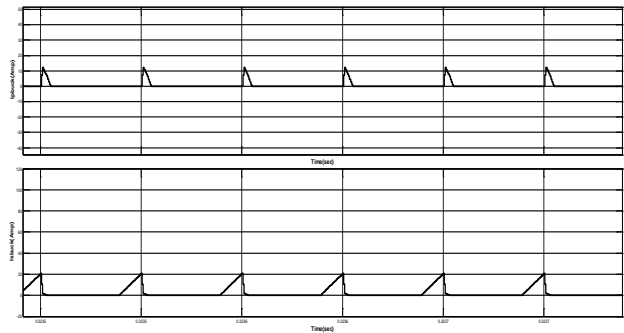


Fig.18. Simulated a) Primary current b) Secondary current in buck mode.

2(d). Buck-boost converter

A bidirectional buck-boost converter is shown in Fig 19. As shown in diagram, two DC sources are connected via an inductor switches and diodes. In forward direction of power flow $V_1, S_1, D_2, Load_1, C_{f1}$ and L conduct and power flow is maintained in forward direction (boost mode). Similarly for reverse direction $V_2, S_2, D_1, Load_2, C_{f2}$ conduct and power flow is maintained in reverse direction (buck mode). Inductor Voltage and inductor current in buck mode of operation is shown in Fig.20. Also inductor voltage and current in boost mode are shown in Fig.21.

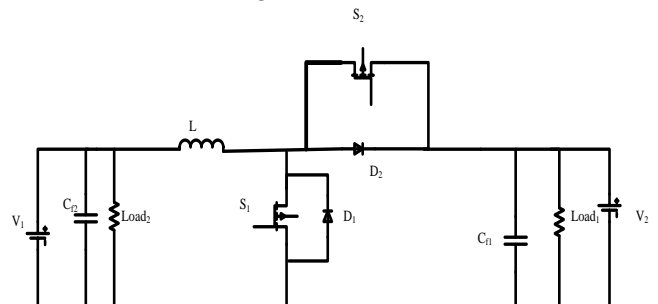


Fig.19. Power circuit diagram of a bidirectional buck-boost converter.

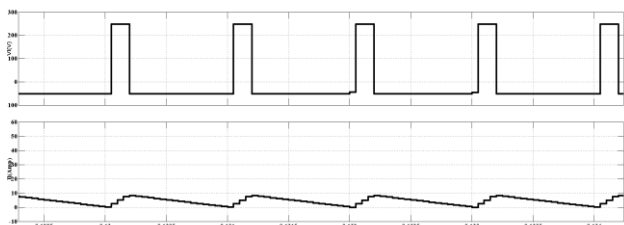


Fig.20. Inductor voltage and inductor current for buck mode of operation.

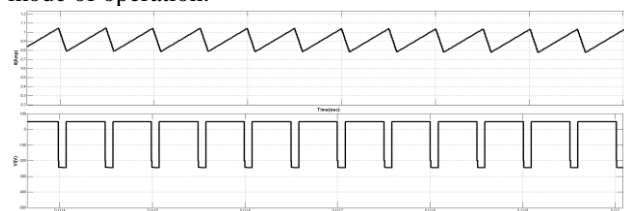


Fig.21. Inductor current and inductor voltage for boost mode of operation

3. Control Techniques

3.a) Dual Active Bridge Converter

Before moving onto the closed loop control used in the present work, first the dependence of transmission power on respective duty ratios (inner and outer phase shift) for all the control strategies is first discussed.

In SPS mode transmitted power is given by

$$P = (NV_1V_2D(1-D))/2f_sL \quad (12)$$

where, V_1 =Primary side voltage, V_2 =Secondary side voltage, N =Transformation ratio of isolation transformer, D =Duty ratio corresponding to outer phase shift between the two bridges
 f_s =Switching frequency, L =Leakage inductance of primary plus referred value of secondary leakage inductance on primary side.

$$C_{input} = (\Delta I_L T_{sw})/8\Delta V_o \quad (13)$$

C_{input} =Input side capacitor value, ΔI_L =Peak to Peak ripple in inductor current

T_{sw} =Total time period($1/f_{sw}$), f_{sw} =switching frequency

$$C_{output} = (I_o DT_{sw})/\Delta V_o \quad (14)$$

C_{output} =Output side capacitor value, I_o =Output current value, D =Duty ratio corresponding to outer phase shift between the two bridges, T_{sw} =Total time period($1/f_{sw}$), f_{sw} =switching frequency, ΔV_o =Peak to Peak ripple in output voltage.

In EPS mode, transmitted power is given by

$$P = NV_1V_2[D_2(1-D_2)+1/2D_1(1-D_1-2D_2)]/2f_sL \quad (15)$$

where, V_1 =Primary side voltage, V_2 =Secondary side voltage, N =Transformation ratio of isolation transformer, D_1 =Inner phase shift duty ratio in primary bridge, D_2 =Outer phase shift duty ratio between primary bridge voltage and secondary bridge voltage, f_s =Switching frequency, L =Leakage inductance of primary plus referred value of secondary leakage inductance on primary side.

After the discussion on transmission power, the closed loop controller used in the closed loop operation is discussed now.

As shown in above Fig-22, in closed loop control of dual active bridge converter, firstly

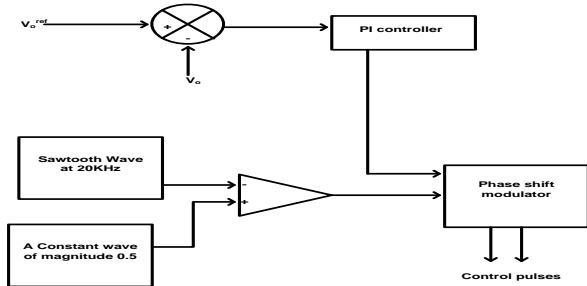


Fig.22., Closed loop control scheme of dual active bridge converter.

the output voltage is sensed, then it is compared with the required reference voltage and the error is processed through a PI controller. After this, a saw tooth wave is compared with a constant of magnitude 0.5. Both are given to the phase shift

modulator to generate gating pulses for the converter. This closed loop controller is used for all the four techniques, only difference is the various phase shifting done through phase shift modulator.

3.b) Flyback Converter

Designing of Flyback converters is done for two modes in both the directions

a) Switch on mode:

$$V_p = L_m \frac{di_{Lm}}{dt} \quad (16)$$

V_p =Primary Voltage, L_m =Magnetizing Inductance,

i_{Lm} =Magnetizing current

Magnetizing current for closed switch operation

$$\Delta i_{Lm_{closed}} = \frac{V_s DT}{L_m} \quad (17)$$

$$V_s = V_p \frac{N_2}{N_1} \quad (18)$$

V_s =Secondary Voltage, $\frac{N_2}{N_1}$ =Turns ratio

$$V_D = -V_o - V_p \frac{N_2}{N_1} \quad (19)$$

V_D =Diode Voltage, V_o =Output Voltage

b) Switch off mode:

$$V_s = -V_o$$

$$V_p = -V_o \frac{N_1}{N_2}$$

$$\frac{di_{Lm}}{dt} = -\frac{V_o N_1}{L_m N_2} \quad (20)$$

$$\Delta i_{Lm_{open}} = \frac{-V_o(1-D)T}{L_m} \frac{N_1}{N_2} \quad (21)$$

V_p =Primary Voltage, L_m =Magnetizing Inductance,

i_{Lm} =Magnetizing current, V_s =Secondary Voltage,

$\frac{N_2}{N_1}$ =Turns ratio, D =Duty Ratio of converter, T =Total Time.

3.c) Buck-boost Converter

Operation of Buck-boost converter can be studied in two modes. Buck mode and Boost mode.

a) Buck mode of operation:

For analysis of circuit we assumed-

- The value of V_o will be treated as constant through the operation it means the ripple value of output voltage is nearly zero or very small.

- Consistent steady state operation of the circuit can be visualized.

The inductor current is related to inductor voltage by

$$di_L/dt = V_L/L = (V_2 - V_1)/L \quad 0 < t < DT \quad (22)$$

After the inductor is charged, it discharges through Diode

$$di_L/dt = V_L/L = -V_1/L \quad DT < t < T \quad (23)$$

$$\Delta I/DT = (V_2 - V_1)/L \quad (24)$$

$$\Delta I = (V_2 - V_1)DT/L, \quad V_1 = DV_2 \quad (25)$$

$$\Delta I = V_2D(1-D)/fL \quad (26)$$

for maximum ripple current, $D=0.5$

$$\Delta I_{max} = V_2/4fL, \quad (27)$$

$$I_{DM} = I_o + \Delta I/2 \quad (28)$$

Here, V_2 =Input voltage for buck mode, V_1 =Output voltage for boost mode, L =Inductor in the circuit, D =Duty Ratio of operation in buck

mode, ΔI =Ripple in inductor current, f =Switching frequency, $T=1/f$, i_L =Inductor Current, I_o =Output current, I_{DM} =Peak Diode current.

The minimum filter capacitance required to reduce its peak to peak ripple voltage below a certain level V_{cp} is given by

$$C_{min} = \Delta I_{max} / 8fV_{cp} \quad (29)$$

b) Boost mode of operation:

The inductor current is related to inductor voltage by

$$di_L/dt = V_L/L = (V_2)/L \quad 0 < t < DT \quad (30)$$

After the inductor is charged, it discharges through Diode

$$di_L/dt = V_L/L = V_2 - V_1/L \quad DT < t < T \quad (31)$$

And the inductor is discharging. By steady-state inductor principle, the average voltage V_L across L is zero.

$$\text{thus giving, } V_2 = V_1/(1-D) \quad (32)$$

The value of Inductor in low side results lower value of ripple current which improves the efficiency.

After the discussion on inductor characteristics, the closed loop controller used in the closed loop operation is discussed now. Same closed loop controller is used in both flyback and buck-boost converter which is shown in Fig.23.

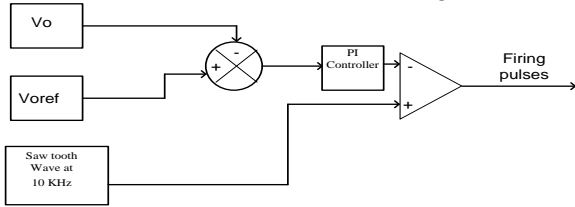


Fig.23. Closed loop control scheme of flyback and buck-boost converter

4. Comparative analysis

4 (a) SPS Technique

The dual active bridge converter is simulated using MATLAB/SIMULINK and SimPowerSystems software. The system parameters are specified in tableIII.

TableIII System parameters

	SPS(forward)	SPS(reverse)
V_{in} (Input voltage)	300V	50V
V_{out} (Output voltage)	50V	10V
C_{in} (Input capacitor)	300 μ F	4500 μ F
C_{out} (Output capacitor)	4500 μ F	300 μ F
L (Leakage inductor)	340 μ H	340 μ H
N (Tranformer ratio)	300:100	100:300
R_{out} (load resistance)	10 Ω	10 Ω
P_{in} (VA)	391	23.32
P_{out} (VA)	252	8.33
Efficiency(%)	64.45	35.677

Dual active bridge converter is modeled and simulated and operated in both forward and reverse mode. As seen in fig.24, first DAB is operated in forward mode, the input voltage is 300V and output is 50V, the transformer ratio is 300:100. In the reverse mode the input is maintained on the low voltage side that is on 100V side and the input voltage is 50V and the output is controlled at 10V. The transformer ratio is 100:300 corresponding to the input side.

Also the efficiency is found to be 64.45% in forward mode while 35.677 % in reverse mode.

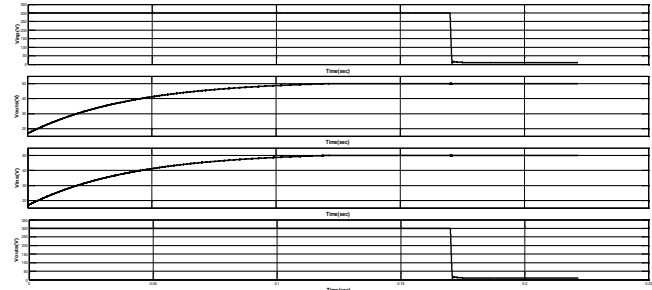


Fig.24. a)Input voltage forward mode(V_{inp} (V)) b)Output Voltage forward mode(V_{outs}) c)Input Voltage reverse mode(V_{ins} (V)) d)Output voltage reverse mode(V_{outp} (V))

4(b) Inherent Soft Switching

Dual active bridge has inherent soft switching capability which can be seen for forward as well as reverse mode, this can be seen in Fig.25 and Fig.26 for both the modes.

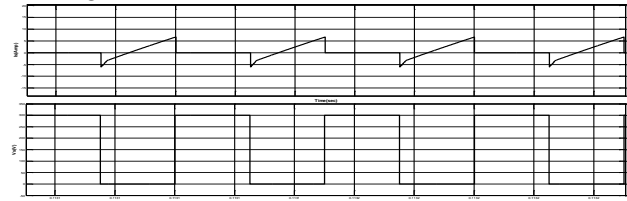


Fig.25. a)Switch Current b)Switch voltage for soft switching in forward mode.

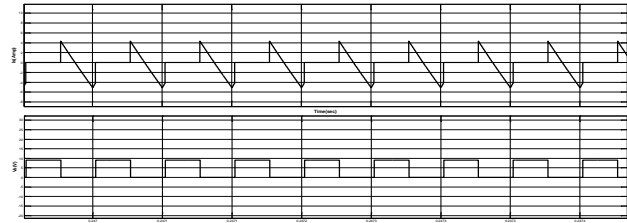


Fig.26. a)Switch Current b)Switch voltage for soft switching in reverse mode.

4 (c) EPS Technique

The dual active bridge converter in EPS mode is simulated using MATLAB/SIMULINK and SimPowerSystem software. The system parameters are specified in tableIV.

TableIV System parameters

	SPS(forward)	SPS(reverse)
V_{in} (Input voltage)	300V	50V
V_{out} (Output voltage)	50V	20V

C_{in} (Input capacitor)	300 μ F	4500 μ F
C_{out} (Output capacitor)	4500 μ F	300 μ F
L(Leakage inductor)	490 μ H	200 μ H
N(Tranformer ratio)	300:100	100:300
R_{out} (load resistance)	10 Ω	10 Ω
P_{in} (VA)	328	83.90
P_{out} (VA)	252	47.52
Efficiency(%)	76.83	56.64

Dual active bridge converter is modeled and simulated and operated in both forward and reverse mode. As seen in Fig.27 first DAB is operated in EPS in forward mode, the input voltage is 300V and output is 50V, the transformer ratio is 300:100. In reverse mode the input is maintained on the low voltage side that is on 100V side and the input voltage is 50V and the output is controlled at 20 V.the transformer ratio is 100:300 corresponding to the input side.

Also the efficiency is found to be 76.83% in forward mode while 56.64 % in reverse mode.

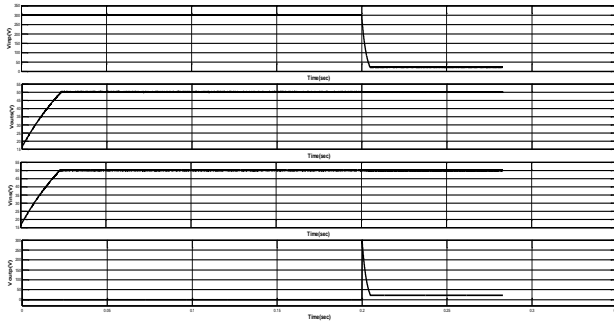


Fig.27. a)Input voltage forward mode(V_{inp} (V)) b)Output Voltage forward mode(V_{outs} (V)) c)Input Voltage reverse mode(V_{ins} (V)) d)Output voltage reverse mode(V_{outp} (V))

4(d) Inherent Soft Switching

Dual active bridge in EPS mode has inherent soft switching capability which can be seen for forward as well as reverse mode, this can be seen in Fig.28 and Fig.29for both the modes.

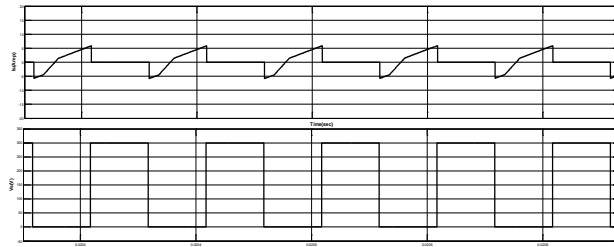


Fig.28. a) Switch Current b)Switch voltage for soft switching in forward mode

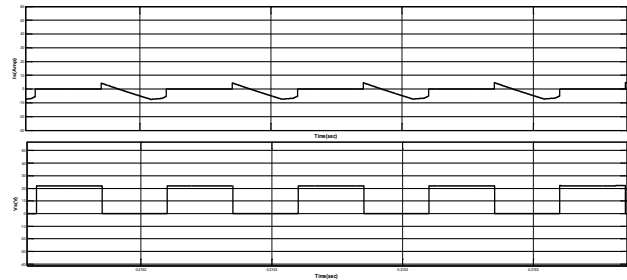


Fig.29. a) Switch Current b)Switch voltage for soft switching in reverse mode.

4(e) Flyback converter

The Flyback converter in bidirectional mode is simulated using MATLAB/SIMULINK and SimPowerSystem software. The system parameters are specified in tableV.

TableV System parameters

	Forward mode	Reverse mode
V_{in} (Input voltage)	100V	300V
V_{out} (Output voltage)	200V	60V
C_{in} (Input capacitor)	500 μ F	500 μ F
C_{out} (Output capacitor)	500 μ F	500 μ F
L(Magnetising inductor)	28.2 mH	28.20 mH
N(Tranformer ratio)	100:300	300:100
R_{out} (load resistance)	100 Ω	100 Ω
P_{in} (VA)	30000	772.5
P_{out} (VA)	867.4	37.85
Efficiency(%)	2.89	4.89

The operation had been discussed earlier now the simulated results are shown Fig.30 and discussed further,

In Fig.30, output of flyback converter in both direction forward as well as reverse is shown.

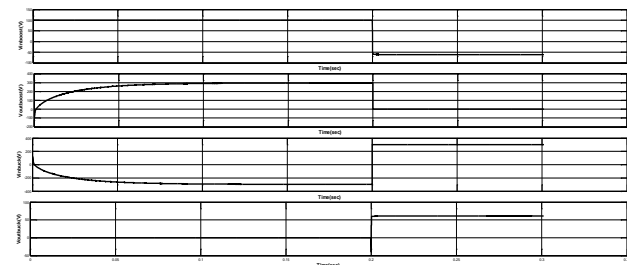


Fig.30. a)Input voltage for boost mode($V_{inboost}$) b)output voltage for boost mode($V_{outboost}$) c)Input voltage for buck mode(V_{inbuck}) d)output voltage for buck mode($V_{outbuck}$).

As shown in the fig.30, input voltage V_1 is 100V till time $t=0.2$ sec and output voltage(load voltage) rises upto 300V.After time $t=0.2$ sec input voltage $V_2=300$ V and output voltage is 60 V.

Flyback converter doesn't show inherent soft switching this can be seen in Fig.31 and Fig.32.

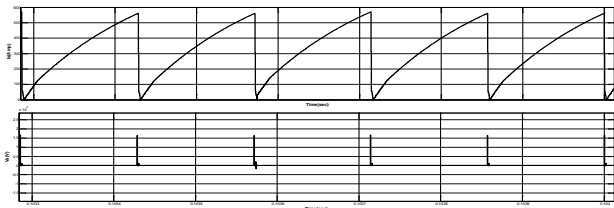


Fig.31 a)Switch Current b)Switch voltage for flyback converter in forward mode.

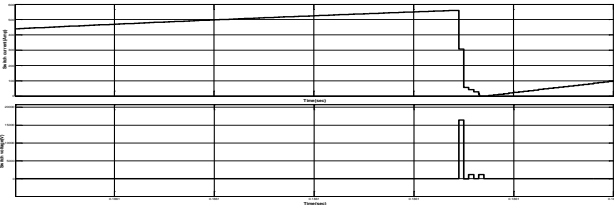


Fig.31 Expanded view of c)Switch Current d)Switch voltage for flyback converter in forward mode



Fig.32 a)Switch Current b)Switch voltage for flyback converter in reverse mode.

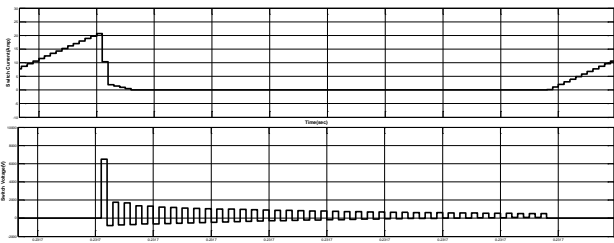


Fig.32 Expanded view of c)Switch Current d)Switch voltage for flyback converter in forward mode

4(e) Buck-boost converter

The Buck-boost converter in bidirectional mode is simulated using MATLAB/SIMULINK and SimPowerSystem software. The system parameters are specified in tableVI.

TableVI System parameters

	Forward mode	Reverse mode
V_{in} (Input voltage)	80V	300V
V_{out} (Output voltage)	300V	50V
C_{in} (Input capacitor)	6000 μ F	50 μ F
C_{out} (Output capacitor)	50 μ F	6000 μ F
L(Magnetising inductor)	10 mH	10 mH
R_{out} (load resistance)	5k Ω	10 Ω
P_{in} (VA)	45.28	225
P_{out} (VA)	18.06	205
Efficiency(%)	39.88	91.11

The operation of buck boost converter had been discussed earlier now the simulated results are

shown Fig.33 and discussed further, In Fig.33, output of buck-boost converter in both direction forward as well as reverse is shown.

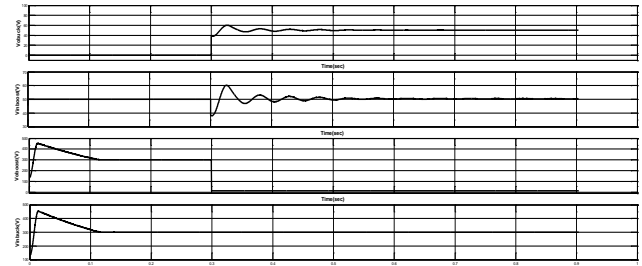


Fig.33a)Output voltage for buck mode(V_{obuck}) b)Input voltage for boost mode($V_{inboost}$) c)Output voltage for boost mode(V_{oboost}) d)input voltage for buck mode(V_{inbuck})

As shown in fig.33, for boost mode input voltage is 50V and output voltage is 300 V. While after time $t=0.3$ sec in buck mode input of buck mode is kept at 300v and output becomes 50V as shown in fig .33.

Buck-boost converter doesn't show inherent soft switching. This can be seen in Fig.34 and Fig.35.

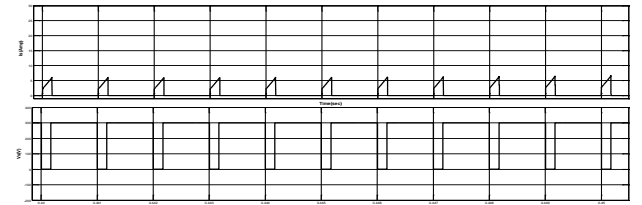


Fig.34.a a)Switch Current b)Switch voltage for buck-boost converter in forward mode

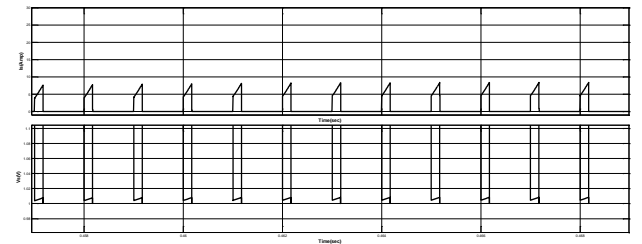


Fig.34.b Expanded view of a)Switch Current b)Switch voltage for buck-boost converter in forward mode.

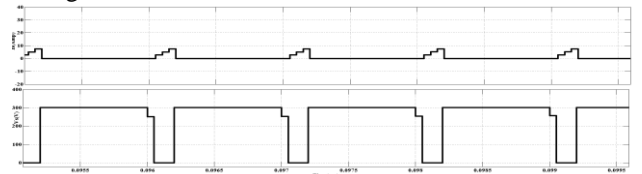


Fig.35.a a)Switch Current b)Switch voltage for buck-boost converter in reverse mode

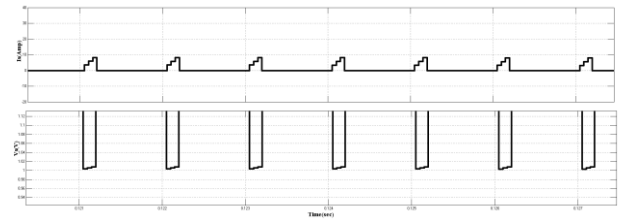


Fig.35.b Expanded view of a)Switch Current b)Switch voltage for buck-boost converter in reverse mode

Conclusions

From the comparative analysis of DAB with SPS and EPS control techniques with flyback as well as buck-boost converter, it can be concluded that DAB with EPS control technique is better than both flyback as well as conventional buck-boost converter. First of all DAB is having inherent soft switching capability, thus making it superior in terms of reduced switching losses as compared to both flyback as well as buck-boost converter. Also the efficiency is higher for bidirectional power flow for both the directions(reverse and forward) respectively for DAB with EPS control technique, while it is quite low for both the directions(forward and reverse respectively) in case of flyback converter. That is why flyback converters cannot be considered for bidirectional power flow at high voltages as its efficiency decreases considerably. In case of conventional bidirectional converters, efficiency is quite high in reverse direction but it decreases in forward direction, that's why DAB with EPS is a better choice in case of bidirectional power flow required in power conversion systems as in case of DAB with SPS control technique efficiency is quite low.

References

- [1] Bai.H., MiC.C and Gargies S., *The Short-Time-Scale Transient Processes in High-Voltage and High-Power Isolated Bidirectional DC-DC Converters*, In: IEEE Transactions on Power Electronics, vol. 23, no. 6, pp. 2648-2656, Nov. 2008.
- [2] ZhaoB., SongQ., Liu.W., Sun.Y., *Overview of Dual-Active Bridge Isolated Bidirectional DC-DC Converter for High Frequency-Link Power Conversion System*, In: IEEE Trans. Power Electron, Vol. 29, No.8, pp. 4091-4106, Aug, 2014.
- [3] Engel S. P., Stieneker M., Soltau N., Rabiee S., Stagge H. and Doncker De W. R., *Comparison of the Modular Multilevel DC Converter and the Dual-Active Bridge Converter for Power Conversion in HVDC and MVDC Grids*, In IEEE Transactions on Power Electronics, vol. 30, no. 1, pp. 124-137, Jan. 2015..
- [4] ShiX., jiangJ., GuoX., *An Efficiency-Optimized Isolated Bidirectional DC-DC Converter with Extended Power Range for Energy Storage Systems in Microgrids*, In: Energies, pp. 27-44, Dec., 2012.
- [5] ZhaoB., SongQ., LiJ., WangY. and LiuW., *Modular Multilevel High-Frequency-Link DC Transformer Based on Dual Active Phase-Shift Principle for Medium-Voltage DC Power Distribution Application*, In: IEEE Transactions on Power Electronics, vol. 32, no. 3, pp. 1779-1791, March 2017
- [6] Inoue S. and Akagi H., *A Bidirectional DC-DC Converter for an Energy Storage System With Galvanic Isolation*, In: IEEE Transactions on Power Electronics, vol. 22, no. 6, pp. 2299-2306, Nov. 2007.
- [7] Jeong K.D., Kim H. S., Baek J. W., Kim Y.J. and Kim J.H., *Dual active bridge converter for Energy Storage System in DC microgrid*, In: IEEE Transportation Electrification Conference and Expo, Asia-Pacific (ITEC Asia-Pacific), Busan, 2016, pp. 152-156.
- [8] Engel S. P., Stieneker M., Soltau N., Rabiee S., Stagge H. and Doncker De W. R., *Dynamic and Balanced Control of Three-Phase High-Power Dual-Active Bridge DC-DC Converters in DC-Grid Applications*, In: IEEE Transactions on Power Electronics, vol. 28, no. 4, pp. 124-137, April. 2013.
- [9] Li X. and Bhat S.K.A., *Analysis and Design of High-Frequency Isolated Dual-Bridge Series Resonant DC/DC Converter*, In: IEEE Transactions on Power Electronics, vol. 25, no. 4, pp. 850-862, April 2010.
- [10] Bai H., Nie Z. and Mi C. C., *Experimental Comparison of Traditional Phase-Shift, Dual-Phase-Shift, and Model-Based Control of Isolated Bidirectional DC-DC Converters*, In: IEEE Transactions on Power Electronics, vol. 25, no. 6, pp. 1444-1449, June 2010.
- [11] Riedel J., Holmes G. D., McGrath P.B. and Teixeira C., *ZVS Soft Switching Boundaries for Dual Active Bridge DC-DC Converters Using Frequency Domain Analysis*, In IEEE Transactions on Power Electronics, vol. 32, no. 4, pp. 3166-3179, April 2017.
- [12] ZhaoB., YuQ. and SunW., *Extended-Phase-Shift Control of Isolated Bidirectional DC-DC Converter for Power Distribution in Microgrid*, In: IEEE Transactions on Power Electronics, vol. 27, no. 11, pp. 4667-4680, Nov. 2012.
- [13] Bai H. and Mi C., *Eliminate reactive power and increase system efficiency of isolated bidirectional dual-active-bridge DC-DC converters using novel dual-phase-shift control*, In: IEEE Trans. Power Electron., vol. 23, no. 6, pp. 2905-2914, Nov, 2008.
- [14] ZhaoB., SongQ. and LiuW., *Power Characterization of Isolated Bidirectional Dual-Active-Bridge DC-DC Converter With Dual-Phase-Shift Control*, In: IEEE Transactions on Power Electronics, vol. 27, no. 9, pp. 4172-4176, Sept. 2012.
- [15] Wen H. and Xiao W., *Bidirectional dual-active-bridge DC-DC converter with triple-phase-shift control*, In: 2013 Twenty-Eighth Annual IEEE Applied Power Electronics Conference and Exposition (APEC), Long Beach, CA, USA, 2013, pp. 1972-

- 1978.
- [16] Weise D.N., Castelino G., Basu K. and Mohan N., *A Single-Stage Dual-Active-Bridge-Based Soft Switched AC-DC Converter With Open-Loop Power Factor Correction and Other Advanced Features*, In IEEE Transactions on Power Electronics, vol. 29, no. 8, pp. 4007-4016, Aug. 2014.
- [17] Kumar A., Bhat H.A. and Singh P.S., *Performance evaluation of fuzzy logic controlled voltage source inverter based unified power quality conditioner for mitigation of voltage and current harmonics*, In: International Conference on Advances in Computing, Communication and Informatics (ICACCI), Jaipur, 2016, pp. 1799-1804
- [18] Dugan C.R., McGranaghan F.M. and Beaty W.H., *Electric Power Systems Quality*. 2ed Edition, McGraw Hill, New York.
- [19] Bollen J.H.M., *Understanding power quality problems voltage sags and interruptions*, IEEE Press, 2000.
- [20] Martinez F.A., Monge B.S., Apruzzese N.J. and Bordonau J., *Operating Principle and Performance Optimization of a Three-Level NPC Dual-Active-Bridge DC-DC Converter*, In: IEEE Transactions on Industrial Electronics, vol. 63, no. 2, pp. 678-690, Feb. 2016.
- [21] Huber L. and Jovanovic H.M., *Forward-flyback converter with current-doubler rectifier: analysis, design, and evaluation results*, In: IEEE Transactions on Power Electronics, vol. 14, no. 1, pp. 184-192, Jan 1999.
- [22] Zhang F. and Yan Y., *Novel Forward-Flyback Hybrid Bidirectional DC-DC Converter*, In: IEEE Transactions on Industrial Electronics, vol. 56, no. 5, pp. 1578-1584, May 2009.
- [23] Li H., Peng Z.F. and Lawler S.J., *A natural ZVS medium-power bidirectional DC-DC converter with minimum number of devices*, In: IEEE Transactions on Industry Applications, vol. 39, no. 2, pp. 525-535, Mar/Apr 2003.
- [24] Lin R.B., Huang L.C. and Lee E.Y., *A symmetrical pulse-width modulation bidirectional DC-DC converter*, In: IET Power Electronics, vol. 1, no. 3, pp. 336-347, September 2008.
- [25] Peng Z.F., Li H., Su J.G. and Lawler S.J., *A new ZVS bidirectional DC-DC converter for fuel cell and battery application*, In: IEEE Transactions on Power Electronics, vol. 19, no. 1, pp. 54-65, Jan. 2004.
- [26] Naayagi T. R., Forsyth J. A. and Shuttleworth R., *High Power Bidirectional DC-DC Converter for Aerospace Applications* In: IEEE Transactions on Power Electronics, vol. 27, no. 11, pp. 4366-4379, Nov. 2012.
- [27] Zhao C., Round D.S. and Kolar W.J., *Full-order averaging modelling of zero-voltage-switching phase-shift bi-directional DC-DC converters*, In: IET Power Electronics, vol. 3, no. 3, pp. 400-410, May 2010.